

Title Page

Dynamics and controls of urban heat sink and island phenomena in a desert city: development of a local climate zone scheme using remotely-sensed inputs

Ahmed K. NASSAR (corresponding author)

Lancaster Environment Centre, Lancaster University, Lancaster, LA1 4YQ, UK;

e-mail: a.nassar@lancaster.ac.uk

Tel.: +44 1524 510237

fax: +44 1524 593985

G. Alan BLACKBURN

Lancaster Environment Centre, Lancaster University, Lancaster, LA1 4YQ, UK;

e-mail: alan.blackburn@lancaster.ac.uk

J. Duncan WHYATT

Lancaster Environment Centre, Lancaster University, Lancaster, LA1 4YQ, UK;

e-mail: d.whyatt@lancaster.ac.uk

ABSTRACT

This study aims to determine the dynamics and controls of Surface Urban Heat Sinks (SUHS) and Surface Urban Heat Islands (SUHI) in desert cities, using Dubai as a case study. A Local Climate Zone (LCZ) schema was developed to subdivide the city into different zones based on similarities in land cover and urban geometry. Proximity to the Gulf Coast was also determined for each LCZ. The LCZs were then used to sample seasonal and daily imagery from the MODIS thermal sensor to determine Land Surface Temperature (LST) variations relative to desert sand. Canonical correlation techniques were then applied to determine which factors explained the variability between urban and desert LST.

Our results indicate that the daytime SUHS effect is greatest during the summer months (typically $\sim 3.0^{\circ}\text{C}$) with the strongest cooling effects in open high-rise zones of the city. In contrast, the night-time SUHI effect is greatest during the winter months (typically $\sim 3.5^{\circ}\text{C}$) with the strongest warming effects in compact mid-rise zones of the city. Proximity to the Arabian Gulf had the largest influence on both SUHS and SUHI phenomena, promoting daytime cooling in the summer months and night-time warming in the winter months. However, other parameters associated with the urban environment such as building height had an influence on daytime cooling, with larger buildings promoting shade and variations in airflow. Likewise, other parameters such as sky view factor contributed to night-time warming, with higher temperatures associated with limited views of the sky.

Keywords: urban heat sink; urban heat island; local climate zones; urban geometry; land cover; Dubai

1. Introduction

The term “Urban Heat Island (UHI)” is mostly associated with air temperature data collected from mobile traverses or weather stations up to two meters above ground level (Emmanuel and Kruger, 2012; Pichierri et al., 2012). However, with the advent of thermal infrared (TIR) remote sensing technology, more studies have investigated surface UHI (SUHI) effects based on differences in land surface temperature (LST) between urban and rural areas measured by various space-borne TIR sensors. Data from space-borne TIR sensors cover larger spatial extents and retrieve temperature measurements for each pixel much more rapidly and cost-effectively than conventional ground-based measurements. Furthermore, remotely-sensed TIR data is particularly useful in areas where the weather stations are sparse or absent altogether (Knight et al., 2010). Although LST is not identical to air temperature, as the former is usually higher than the latter (US EPA, 2008; Yuan and Bauer, 2007), a study by Coutts and Harris (2012) revealed that trends in LST derived from remotely sensed imagery were similar to trends in air temperature, albeit with differences in absolute values.

While many factors affect the formation of a SUHI and its intensity, such as local weather conditions and geographical location, a key contributor is urbanization where the natural land cover is replaced by impervious surfaces (e.g. Imhoff et al., 2010; Rhee et al., 2014; Weng, 2001). As a consequence of urbanization, the evapotranspiration, thermal properties and wind flow of the landscape is altered, which can lead to an increase in surface temperatures in cities (Kato and Yamaguchi, 2005; US EPA, 2008). The increase in impervious surfaces leads to the increase of absorption of solar energy and its conversion to sensible heat rather than latent heat. This is evident when compared to rural areas through the increase of heat storage in urban areas

from the combination of two properties: thermal conductivity and heat capacity (Gartland, 2008; Obiakor et al., 2012).

For cities in desert environments, a SUHI has been observed during the night while a surface urban heat sink (SUHS) has been observed during the day, where urban areas exhibit lower temperatures than rural areas (Frey et al., 2007; Lazzarini et al., 2013). Previous remote sensing studies in desert cities have focused on investigating the direct relationship between land surface temperature and surface cover (i.e. impervious surface and vegetation) from a two-dimensional perspective (Frey et al., 2007; Lazzarini et al., 2013). However, no research has thoroughly examined the effects of the three-dimensional urban geometry on the formation of SUHS and SUHI phenomena in desert cities. Indeed, urban geometry is considered a significant factor in determining the temperature distribution within cities (Unger, 2009; Voogt and Oke, 2003). This investigation into the effects of urban geometry and land cover type on surface temperature variation is motivated by previous studies in desert cities that have found that even areas lacking vegetation and being largely composed of impervious surfaces exhibit lower day time surface temperatures than surrounding rural areas (Frey et al., 2007, Imhoff et al., 2010). Furthermore, proximity to large water bodies has not been considered in previous studies of SUHS and SUHI phenomena in coastal desert cities (Frey et al., 2007; Lazzarini et al., 2013) in spite of its recognized importance (e.g. Coseo and Larsen, 2014).

1.1. Local Climate Zones in the urban environment

Stewart and Oke (2012) developed a climate-based classification system called 'Local Climate Zones' (LCZs) in order to standardize the classification and sampling of field sites in urban heat island studies and facilitate the comparison between several sites within the urban

landscape. Typically, the study area is classified into a number of LCZs, each with a diameter ranging from hundreds of meters to several kilometres that share relatively similar geometry and land cover characteristics

A recent study by Stewart et al. (2014) based on three temperate cities concluded that thermal contrasts do exist among different LCZs and are governed primarily by urban geometry, tree heights and proportion of pervious surfaces. Thus, the LCZ system was deemed useful to investigate the UHI among various locations within the cities. Several UHI studies have adopted the LCZ classification system based on air temperature measurements using fixed or mobile weather stations (Alexander and Mills, 2014; Leconte et al., 2015; Siu and Hart, 2013). Others have proposed various methods to classify the urban environment into LCZs and map their distribution across a study site using inputs from remote sensing and other spatial data using GIS techniques (e.g. Bechtel and Daneke 2012; Lelovics et al., 2014), although this was done for different reasons than the research presented in this paper. This study uses a similar approach to classifying and mapping LCZs by using the available spatial data for the study site and developing and applying an appropriate classification method to this data. The boundaries of the mapped LCZs were then used to explore the spatial and temporal differences in LST measured from remotely-sensed TIR data.

1.2. Aim and objectives

The aim of this study was to elucidate the dynamics and controls of SUHS and SUHI phenomena in the desert city of Dubai. In order to achieve this aim three objectives were addressed: (i) to develop a technique to categorize the urban environment of Dubai into LCZs in accordance with the LCZ classification system; (ii) to study the diurnal and seasonal dynamics of

the SUHS and SUHI in the LCZs using remotely-sensed thermal imagery; and (iii) to investigate the impact of different physical variables (related to urban geometry, proximity to the Arabian Gulf and land cover properties) on the temporal dynamics of the SUHI and SUHS phenomena.

2. Study Area

Situated on the Arabian Gulf, Dubai emirate (25° 16'N, 55° 20'E) is considered one of the fastest growing cities in the Middle East and has been transformed into a city of global stature (Elsheshtawy, 2010). The total administration area of the emirate before the development of the islands was 3885 km² and the population reached 2,213,000 inhabitants in 2013 (Dubai Statistical Centre, 2013).

Dubai Creek divides the city into Deira to the east and Bur Dubai to the west forming bi-central districts comprised of high-density buildings. Bur Dubai is generally known for its modern high-rise buildings, however, low-rise to mid-rise building blocks are spreading in both directions from the Creek. In the last two decades, the physical size of the urban area has grown dramatically both horizontally and vertically and the desert has been transformed into residential, commercial, sports and tourism projects. The total urban area has increased horizontally to approximately 560 km² in year 2011 (Nassar et al., 2014) while vertically, 96 buildings in Dubai are greater than 150m in height. In 2011, approximately 14% of the Emirate was covered by impervious surfaces (buildings, roads, walking-ways and parking lots) and 1.1% by vegetation (Nassar et al., 2014).

Due to the diversity of building heights in Dubai and the systematic urban planning process, large discrete blocks of different urban land use types and building heights have been created, making this an interesting study site for investigating the impact of urban geometry on

SUHS and SUHI effects. For example, residential areas are usually comprised of low to midrise buildings; mixed land use areas (commercial and residential combined) are usually comprised of mid to high-rise buildings while industrial areas are comprised of low-rise buildings.

Dubai is built upon flat terrain and experiences a hot and arid climate. Desert sand is the main land cover type in the emirate. The warmest months in Dubai are July and August with an average maximum temperature of 43°C and an average minimum of 33°C, while the coldest months are January and February with an average maximum of 26°C and an average minimum of 16°C (Dubai Statistical Centre, 2014).

Our specific study area covers the main urban areas in Dubai which consist of a variety of urban structures, configurations and land cover types covering an area of 450km² (Fig. 1). The study area was also chosen based on the availability of building footprint data for the city which were used to compute urban geometry parameters. It has also been designed to exclude the coastal strip (1km) in order to avoid the problem of mixed pixels (land-water) in the remotely-sensed imagery which is a confounding factor in thermal studies of coastal regions (Lazzarini et al., 2013).



Figure 1. Overview map of the study area and the Arabian Gulf, Dubai based on a Landsat 8 scene from 2013 (Latitude: 25° 16'N; longitude: 55° 20'E).

3. Materials and Methods

To achieve the aim and objectives of the study, the following steps were taken: (1) derivation of urban geometry and land cover parameters from several datasets, (2) selection of LCZs based on the derived parameters according to the LCZ classification system, (3) LST retrieval using Dubai's LCZs based on day and night-time satellite imagery, (4) investigation of the SUHS and SUHI magnitudes diurnally and seasonally for each LCZ, and (5) determination of the

relationships between different physical variables and the seasonal SUHS and SUHI variations during day and night-time. The schema in Figure 2 lists the major steps of the methodology.

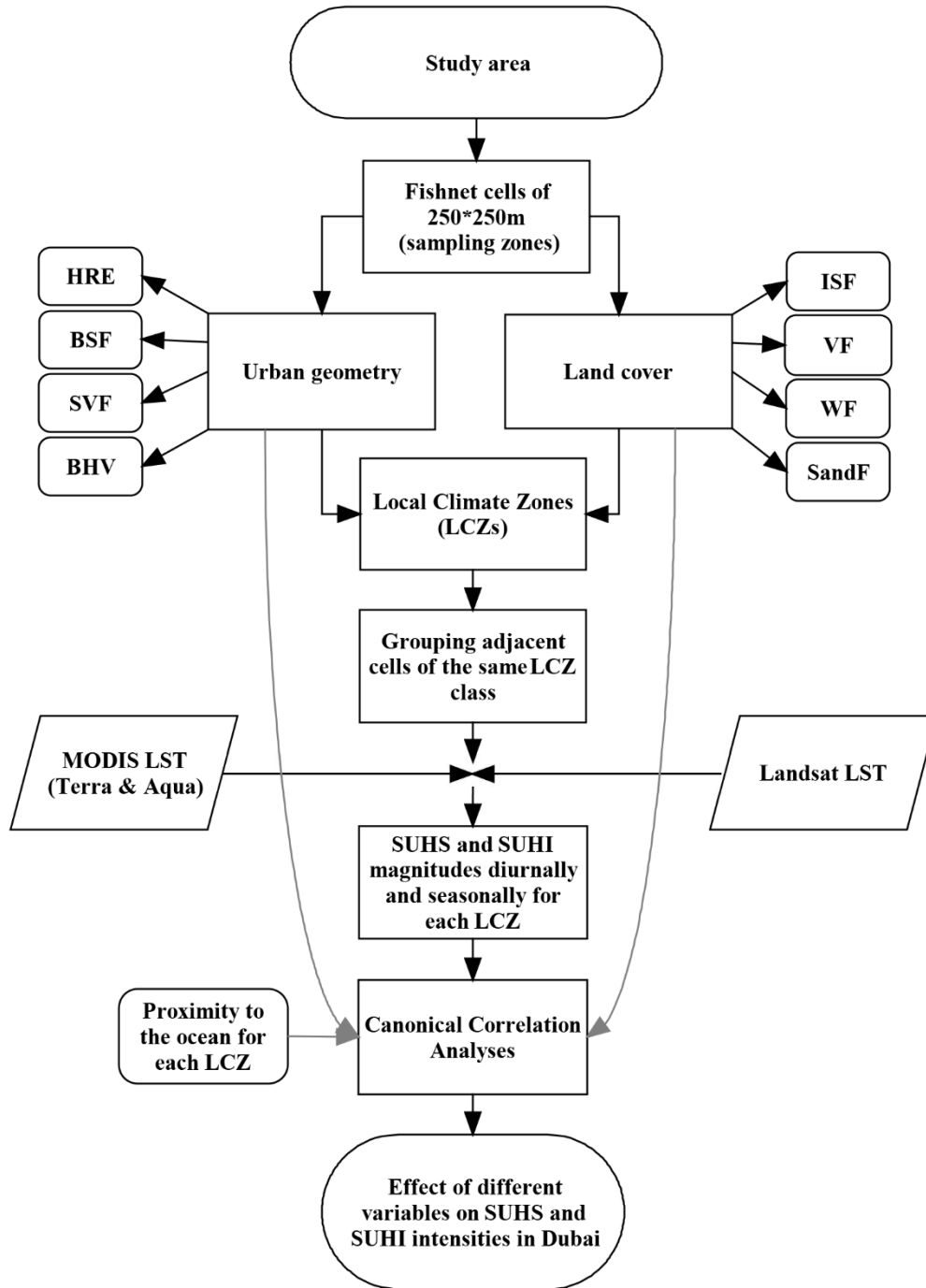


Figure 2. Flowchart showing the main stages of LCZs selection process and analysis. HRE: height of roughness elements, BSF: building surface fraction, SVF: sky view factor, BHV: building height

variation, ISF: impervious surface fraction, VF: vegetation fraction, WF: water fraction, SandF: sand fraction.

3.1. Local Climate Zone parameters

The Stewart and Oke (2012) classification system defines 17 LCZs based on their geometrical, land cover and thermal characteristics (Table 1). The LCZs are categorized according to the geometrical properties: sky view factor (SVF), aspect ratio (h/w), building surface fraction (BSF) and height of roughness elements (HRE). They are also categorized according to the land cover properties: impervious surface fraction (ISF) and pervious surface fraction (PSF). The LCZs are also categorized according to their thermal, radiative, and metabolic properties such as surface admittance and anthropogenic heat output. For the full list of properties of each LCZ consult Stewart and Oke (2012, p1885-1887).

Table 1.

LCZ classification system (source: Stewart and Oke, 2012)

Urban classes	LCZ code	Land cover classes	LCZ code
Compact high-rise	LCZ 1	Dense trees	LCZ A
Compact mid-rise	LCZ 2	Scattered trees	LCZ B
Compact low-rise	LCZ 3	Bush, scrub	LCZ C
Open high-rise	LCZ 4	Low plants	LCZ D
Open mid-rise	LCZ 5	Bare rock or paved	LCZ E
Open low-rise	LCZ 6	Bare soil or sand	LCZ F
Lightweight low-rise	LCZ 7	Water	LCZ G
Large low-rise	LCZ 8		
Sparsely built	LCZ 9		
Heavy industry	LCZ 10		

Based on the parameters used to classify LCZs in Stewart and Oke (2012) and other parameters used in previous UHI studies, we determined nine different parameters for the LCZ classification of Dubai based on the availability of datasets for the study site: height of roughness elements (HRE); building surface fraction (BSF); sky view factor (SVF); building height variation (BHV); impervious surface fraction (ISF); vegetation fraction (VF); water fraction (WF); sand fraction (SandF); and proximity to the ocean. Out of the nine parameters, five

parameters relating to urban geometry and land cover type (HRE, BSF, SVF, ISF and PSF: Pervious Surface Fraction) were utilized from the Stewart and Oke classification system (2012). In their system, pervious surface fraction (PSF) is considered a single parameter, however, it actually combines three pervious surfaces: vegetation, water and bare soil, each of which has a different effect on surface temperature. Therefore, in our study, PSF was divided into three separate parameters: vegetation, inland water and sand. In Dubai, inland water consists of small recreational bodies (e.g. swimming pools, small lakes on golf courses) that cover only 0.3% of our study area, nevertheless it has been treated as a separate parameter. Sand is likely to play an important role in surface thermal differences as it is the dominant land cover type in desert environments.

In addition, we added a building height variations (BHV) parameter because a group of buildings with varying heights tends to increase wind circulation within urban areas which helps in air and surface cooling (Johansson and Emmanuel, 2006). Furthermore, Coseo and Larsen (2014) have used proximity to water bodies to understand the variations in UHI intensity across a city. Urban areas that are close to large water bodies tend to have lower UHI intensity because cold breezes that are generated from water bodies convect heat away from urban surfaces, thus potentially mitigating the effects of UHI in cities (Oda and Kanda, 2009; US EPA, 2008). The sea-breeze effect is pronounced during daytime due to the difference in air pressure over land and water caused by the variation in surface temperatures, while at night an inverse land-breeze system is formed (Freitas et al., 2007). Hence, the proximity to the ocean was deemed as an important parameter for Dubai due to the location of the city on the coastline of the Arabian Gulf.

3.1.1. Urban Geometry Parameters

In order to compute the urban geometry parameters we utilized a vector format GIS layer for Dubai which contains approximately 175,000 individual building ‘footprints’ (polygons) and associated attributes (including height) acquired from Dubai Municipality. The buildings data were spatially precise; however, in order to evaluate height accuracy a random sample of 50 buildings were selected from an independent database (specifically of tall buildings >100m but this was the only available independent height data for Dubai) from the Council on Tall Buildings and Urban Habitat (Skyscraper Center, 2016) and the heights of these samples were compared to the heights for the corresponding buildings in the municipality data. The results show consistent building heights between the two sources (RMSE = 2.45m). Hence, the municipality data were subsequently used to compute four urban geometry parameters.

SVF (Sky View Factor) is a widely used parameter in urban thermal studies and is considered as an essential controlling factor of the UHI effect. It represents a dimensionless quantity of visible sky (Hwang et al., 2011). This parameter represents the amount of solar radiation that reaches or leaves the surface, and thus has an impact of surface heating and cooling during the day and night (Heldens et al., 2013). This geometric variable is preferred over other geometric variables such as the aspect ratio because it can describe the complex urban environment more efficiently (Johnson and Watson, 1984). Although many methods have been used to compute SVF, ranging from fish-eye photos to computer modeling software, the vast majority of these methods rely on computing SVF for specific ground locations and do not derive SVF for building rooftop locations. Since this study examines the impact of SVF on LST from a remote sensing perspective, the value for each ground and rooftop pixel should be computed. For this reason, the SVF was computed using a model developed by Zakšek et al.

(2011). Using the three dimensional buildings data as an input, a continuous SVF map for the entire urban environment was generated at 1m pixel resolution. The SVF is stored for each pixel with values ranging from 0-1 (0 denotes that no sky is visible while 1 indicates that the entire sky hemisphere is visible) (Fig. 3).



Figure 3. Sky view factor of a small sample area in Dubai at 1m resolution derived using a raster based model (Latitude: 25°16'23.67"N; longitude: 55°18'44.59"E).

HRE (Height of Roughness Elements) is defined as the heights of buildings and trees in meters. We excluded tree heights from our parameter due to a lack of data and because there are few trees in Dubai in any case with the exception of parks and farms. The BHV (Building Height Variation) parameter is computed based on the variation or distribution of building heights in a given area compared to the mean for that area. The higher the value, the greater the variation in height, with zero representing buildings of uniform height. The standard deviation was used

because it is a more reliable measure of variation, and is less susceptible to outliers. Finally, BSF (Building Surface Fraction) is the horizontal area of building footprints per unit area of ground.

This was computed using the building footprint polygons.

3.1.2. Land Cover Parameters

In this study, three land cover parameters were derived from large-scale land cover maps that provide a detailed representation of urban areas of Dubai (Source: Dubai Municipality). For the purposes of this study roads, walkways and car parking lots were merged into a single category of impervious surfaces while vegetation, inland water and sand were maintained as separate land cover categories. An accuracy assessment was undertaken for the land cover map using 150 random samples (map and reference pairs). The reference samples were identified through manual interpretation of a Dubai Sat-1 image at spatial resolution of 2.5m (pan-sharpened) from 2013 acquired from Emirates Institution for Advanced Science and Technology. This analysis revealed that the municipality land cover map had an overall accuracy of 98% and was therefore suitable for use in this study.

3.2. Land Surface Temperature Retrieval

With the availability of various TIR sensors on board different satellite platforms, a choice has to be made between using thermal data at high spatial resolution or high temporal resolution. Similarly, a choice has to be made between using sensors that acquire data at different stages of the diurnal cycle. For example, Landsat 8 and ASTER sensors provide medium spatial resolution thermal data (100m and 90m respectively) over a relatively long revisit time (16 days) whilst MODIS and AVHRR sensors provide coarser resolution thermal data (1km) over short

revisit times of less than 24 hours. It is not currently possible to acquire LST data at both high spatial and temporal resolution (Sattari & Hashim, 2014).

In this study, LST data were retrieved from two satellites which have been widely used in thermal studies due to their favorable spatial and temporal resolution and free availability to the research community: (i) MODIS (Moderate Resolution Imaging Spectroradiometer) TIR data with low spatial resolution of 1km and four times daily revisit time; (ii) Landsat 8 TIR data with medium spatial resolution of 100m (resampled to 30 meters to match multispectral bands) and 16-day revisit time.

MODIS is the instrument on board the Terra (Launched in late 1999) and Aqua (launched in mid-2002) satellites. Terra and Aqua orbits generate different overpass times. Terra acquires data for Dubai at approximately 11 a.m. (Gulf Standard Time; GST) and 11 p.m. (GST), while Aqua acquires data for Dubai at approximately 2 p.m. (GST) and 2 a.m. (GST). MODIS data have been widely used in SUHI studies because of the ability to provide LST measurements four times daily facilitating study of the diurnal variations in SUHI (e.g. Cui and Foy, 2012; Lazzarini et al., 2013). MODIS bands 31 and 32 are used to retrieve 1km LST data by using the generalized split-window algorithm which corrects both atmospheric effects and surface emissivity (Wan and Dozier, 1996). For this study eight-day composite 1km LST MODIS Terra (MOD11A2) and Aqua (MYD11A2) V5 products were acquired for year 2013. These LST data were derived from daily 1km LST products MOD/MYD_11A1 and the eight-day image compositing removes any effects of cloud cover.

Landsat 8 was launched in early 2013. Images are available for Dubai from 13-April-2013 and the local crossing time is approximately 10:40 a.m. (GST). Although the Landsat 8 Thermal Infrared Sensor (TIRS) has two spectrally adjacent thermal bands (bands 10 and 11)

which are suitable for the split window techniques for atmospheric correction and LST retrieval, the Landsat science team does not recommend using band 11 in split-window techniques due to the larger calibration uncertainty associated with it (USGS, 2014). Thus, a single window technique based on band 10 is preferred at this stage. A total of nine cloud free scenes covering the study site were available between the period of April to December 2013 and were acquired from the NASA archive. The single window method from Yuan and Bauer (2007) was used to derive LST from TIR band 10 which takes into account the atmospheric parameters and surface emissivity (Fig. 4). Both Landsat and MODIS data were georeferenced to the Dubai municipality land cover map in order to perform the subsequent analysis.

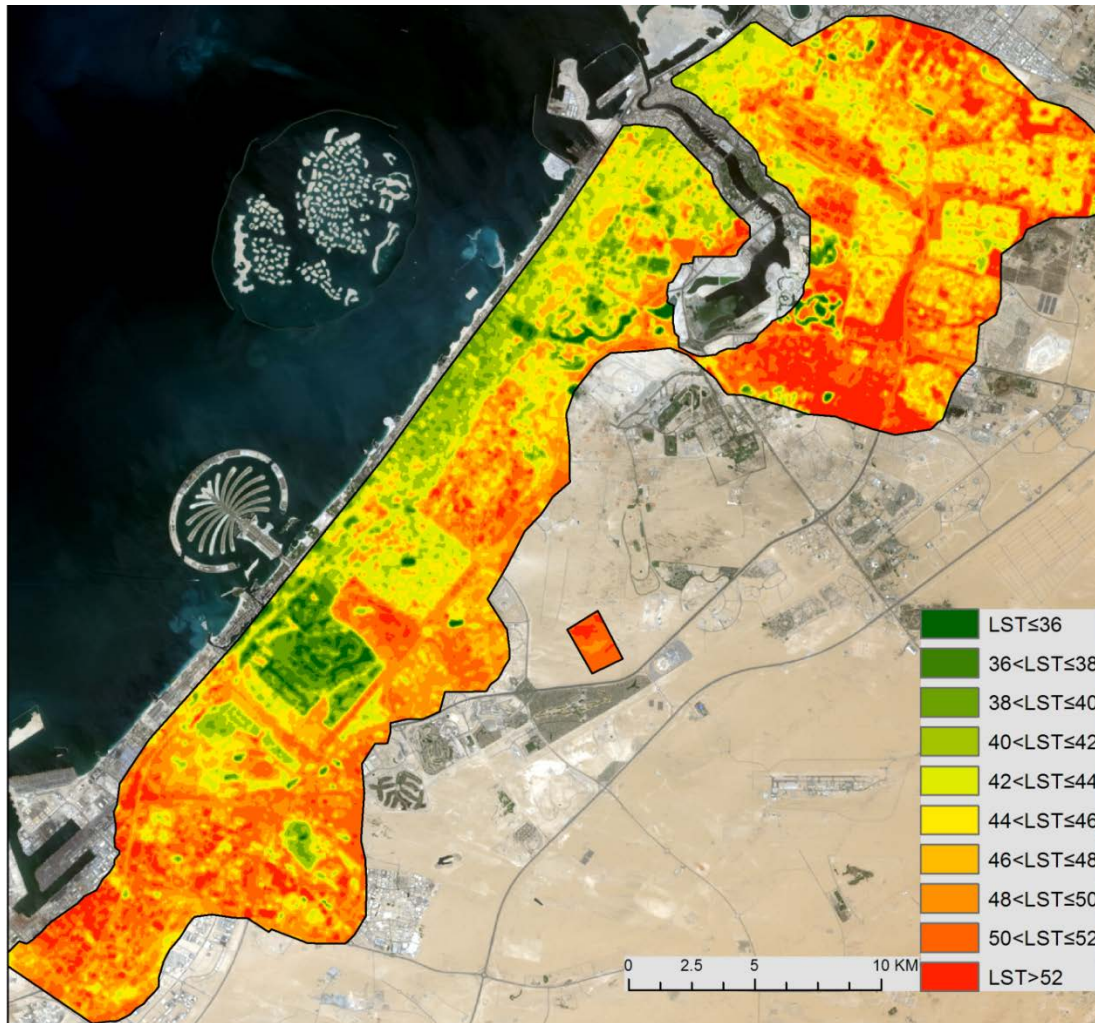


Figure 4. Example of daytime LST in $^{\circ}\text{C}$ image for Dubai acquired on July 18 2013 at 10:40 a.m. (GST) using Landsat 8 TIRS (Latitude: $25^{\circ} 16' \text{N}$; longitude: $55^{\circ} 20' \text{E}$).

3.3. LCZs classification in Dubai & LCZs sampling technique

The study area (Fig.1) was subdivided into a regular grid ('fishnet') of $250 \times 250 \text{m}$ cells. This was used to compute the geometry and land cover parameters for each cell in order to classify the study area into LCZs. As a result, 6750 cells were produced including a detached area of desert sand cells (4km^2) to represent the main non-urban land cover type of Dubai. The desert sand zone (LCZ_{Sand}) was used for both LST normalization purposes and to represent the LST of the rural area for comparison with urban LCZs.

The HRE parameter was used as the primary criterion for LCZ classification and the average building height per grid cell was computed. Each cell was then categorized into one of three classes according to the LCZ classification system: high-rise, mid-rise and low-rise cells (see Table 2 for height ranges). The BSF parameter was then used to categorize the cells in terms of compactness (open or compact). This was followed by a classification of ISF and PSF based on the proportion of vegetation, inland water and sand per grid cell. The SVF parameter was not employed in the selection process because in Stewart and Oke (2012) the SVF was based on SVF measured from ground observations. Nevertheless, the SVF for each cell was computed for subsequent analyses. Proximity to the ocean was then calculated using the Euclidian distance from the centroid of each grid cell to the coastline of the Arabian Gulf.

Finally, groups of at least four adjacent cells of the same LCZ class were identified and all other cells were excluded to comply with Stewart and Oke's recommendation that each LCZ should occupy an area of at least 500-1000m² and also to facilitate comparison of the LCZs with MODIS LST data at a spatial resolution of 1km². As a result of the selection criteria and the computed parameters, seven LCZs were derived, the boundaries of which are illustrated in Fig. 5. Note that the areas of the study site not mapped as an LCZ did not meet the selection criteria of our classification system and were excluded from the subsequent analysis. The detailed characteristics of Dubai's urban LCZs in terms of configuration, land cover and construction materials are given in Tables 2 and 3.

Following the classification process, the boundaries of the areas covered by each LCZ type were overlaid on the MODIS data and used to extract data on the average daytime LST (11 a.m. and 2 p.m.) and night-time LST (11 p.m. and 2 a.m.) for each LCZ. Similarly, the average daytime LST from Landsat (10:40 a.m.) was also extracted for each LCZ.

In order to study the magnitude of the temperature differences amongst the various LCZs, the differences between LST for the six urban LCZs and LST for desert sand (using this as a reference) were computed using the following (adapted from Stewart et al., 2014):

$$\Delta LST = LST LCZ_i - LST LCZ_{Sand} \quad (1)$$

Where, $LST LCZ_i$ is the average land surface temperature for each urban LCZ where i can be CMR, LLR, OHR, OLR, OMR, SB; and $LST LCZ_{Sand}$ is the average land surface temperature for the desert sand zone. When ΔLST is a positive value this represents a SUHI and when negative this represents a SUHS.

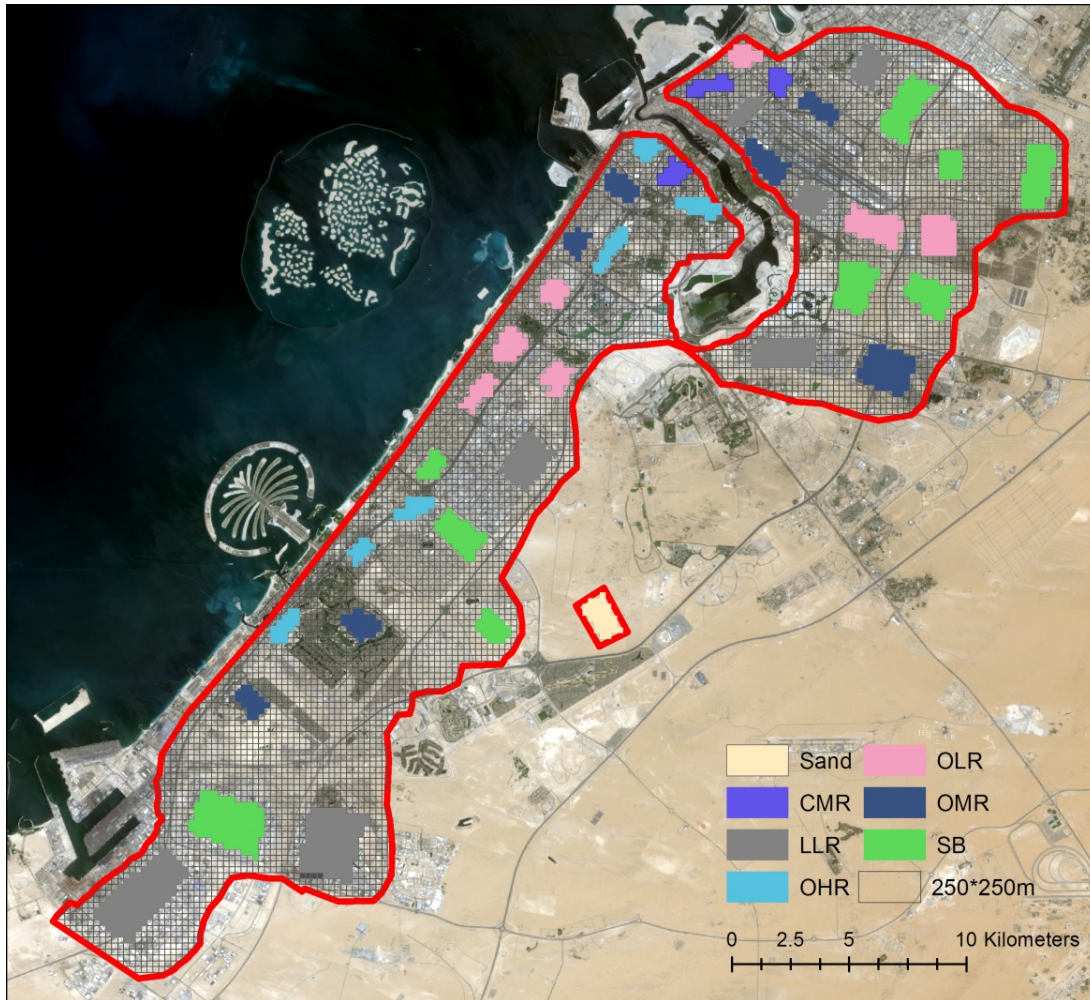


Figure 5. The fishnet of 250*250m cells and the obtained LCZ map of Dubai with a Landsat 8 scene from 2013 displayed in the background (Latitude: 25° 16'N; longitude: 55° 20'E). CMR= compact mid-rise, LLR= large low-rise, OHR= open high-rise, OLR= open low-rise, OMR= open mid-rise, SB= sparsely built.

Table 2.

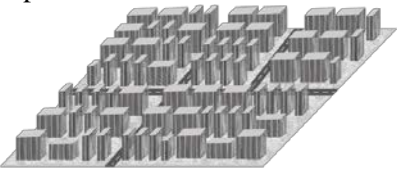
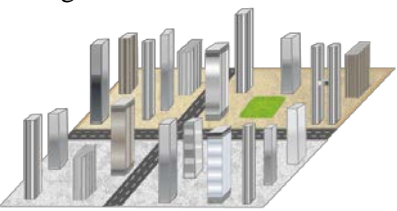

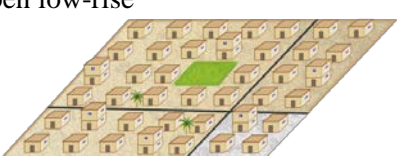
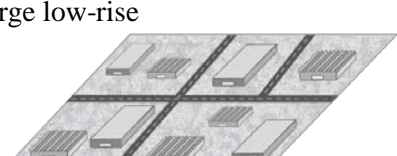
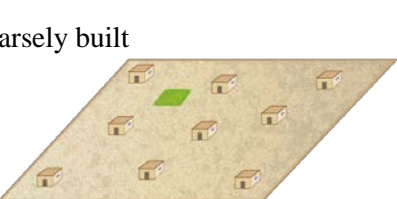
Urban geometry and land cover properties of LCZs as originally defined by Stewart and Oke, (2012) and as adapted for Dubai in this study.

LCZs	HRE (m)	HRE_{Dubai}	%BSF	BSF_{Dubai}	SVF	SVF_{Dubai}	%ISF	ISF_{Dubai}	%PSF	PSF_{Dubai}	BHV_{Dubai}	Proximity to the ocean (km)
CMR	10-25	18-25 (22)	40-70	49-64 (56)	0.3–0.6	0.70-0.80 (.73)	30-50	34-36 (35)	<20	02-16 (9)	5-8 (7)	1.5-3 (2.3)
OHR	>25	43–85(65)	20-40	25-33 (29)	0.5–0.7	0.60-0.75 (.72)	30-40	32-39 (35)	30-40	32-41 (36)	12-20 (15)	1.6-5 (2.5)
OMR	10-25	12-23 (19.4)	20-40	21-34 (26)	0.5–0.8	0.70-0.85 (.76)	30-50	26-48 (33)	20-40	17-50 (41)	4-8 (6)	1-15 (7)
OLR	3-10	6-12 (8)	20-40	22-34 (27)	0.6–0.9	0.70-0.90 (.83)	20-50	17-29 (21)	30-60	41-57 (52)	3-5 (3.5)	1.1-13 (6)
LLR	3-10	5-9 (7)	30-50	35-51 (40)	>0.7	0.84-0.91 (.87)	40-50	46-53 (51)	<20	4-15 (9)	2-4 (2.9)	3-11 (7)
SB	3-10	6-11 (7.8)	10-20	13-19 (16)	>0.8	0.88-0.95 (.93)	<20	08-14 (10)	60-80	67-79 (74)	2-4 (2.6)	2-14 (9)

Note: values between parentheses represent the average calculated values.

Table 3.

The characteristics of the urban LCZ classification for Dubai in terms of configuration, land cover and construction materials.

Urban local climate zones in Dubai	Configuration & land cover	Construction materials
<p>Compact mid-rise</p> 	<p>Dense mix of midrise buildings with medium height variations and relatively narrow roads. Sparse or no pervious cover types.</p>	<p>Bricks, concrete, steel and some glass. Pavements of asphalt and concrete for roadways and walkways.</p>
<p>Open high-rise</p> 	<p>Open configuration of tall buildings with large height variations and wide roads. Plenty of pervious land covers of sand and some vegetation.</p>	<p>Comprised of mostly modern high-rise buildings made from glass, steel and other metal construction materials with mostly sharp edges.</p>
<p>Open mid-rise</p> 	<p>Open configuration of mid-rise buildings with medium height variations. Plenty of pervious land covers of sand and some of vegetation and trees.</p>	<p>Bricks, concrete, steel and some glass. Pavements of asphalt and concrete for roadways and walkways.</p>
<p>Open low-rise</p> 	<p>Open configuration of low-rise buildings with moderate height variations and narrow roads. Plenty of pervious land covers of sand and some vegetation and trees.</p>	<p>Found mostly in residential areas and made of bricks, stone and concrete. Pavements of asphalt, concrete and sand for roadways and walkways.</p>
<p>Large low-rise</p> 	<p>Open configuration of large low-rise buildings with low height variations. Mainly paved land cover and no or very sparse vegetation.</p>	<p>Found mainly in industrial areas and made mostly of metal corrugated sheets and steel hangers. Pavements of asphalt and concrete for roadways and walkways.</p>
<p>Sparsely built</p> 	<p>Sparse configuration of low-rise buildings with low height variations. Abundance of sand as the major land cover type.</p>	<p>Found mainly in residential areas and made of bricks, stone and concrete. Pavements of sand and some asphalt for roadways and walkways.</p>

3.4. Multivariate Correlation Analysis

In order to investigate the factors influencing the SUHS and SUHI variations amongst the different LCZs we performed a canonical correlation analysis. Canonical correlation analysis is a multivariate analysis technique that is used to analyze the relationship between two sets of variables, a predictor set and a criterion set (Guarino, 2004). In the case of our study, this technique is used to investigate the impact of physical variables (urban geometry, land cover and proximity to the ocean) on the diurnal and seasonal variations in the magnitude of SUHS and SUHI phenomena.

Despite the similarities with bivariate and multiple regression analysis, canonical correlation overcomes the limitations of other techniques (Tabachnick and Fidell, 2012). The bivariate technique can handle a relationship between two variables, while the canonical technique can handle two sets of variables. Furthermore, the major difference between the canonical technique and multiple regression analysis is that in the canonical the relationships between more than one variable as predictors and more than one variable as criteria can be examined simultaneously. Furthermore, canonical correlation is preferable to principal components analysis, which is primarily applicable to the analysis of a single set of variables.

In the statistical analysis only MODIS data were used due to the limited number of Landsat scenes available and because Landsat data are only acquired at one time during the day compared to 4 times daily for MODIS. Therefore, MODIS data were used because they capture more comprehensively the SUHS and SUHI variations diurnally and seasonally, though clearly this is at the expense of using lower spatial resolution data than that of Landsat. For the statistical analysis four variables were used to capture the diurnal and seasonal dynamics of the SUHS effect, these were the magnitude of the SUHS at 11 a.m. and at 2 p.m. in summer and at 11 a.m.

and 2 p.m. in winter. Likewise, the magnitude of the SUHI at 11 p.m. and at 2 a.m. in summer and at 11 p.m. and 2 a.m. in winter to characterise the dynamics of the SUHI effect.

Inland water fraction was not included in the statistical analysis because it is not a valid factor statistically as only 4 out of 39 areas of the classified LCZs contained water bodies. Therefore, the canonical technique was used in this study to investigate the correlation between a set of predictor physical variables from one side and a set of criteria variables related to SUHS or SUHI intensity on the other side. Given the characteristics of our data, the canonical correlation was the most appropriate method of analysis (Tabachnick and Fidell, 2012; p. 571).

4. Results

4.1. Dynamics of the surface urban heat sink and heat island phenomena

The eight-day MODIS data from both Terra and Aqua were used to observe the temporal variations of LST amongst the six urban LCZs and the desert sand zone in Dubai. Subsequently, the magnitude of the SUHI or SUHS for each LCZ was computed and this data was used to investigate the temporal trends based on 8-day, monthly and seasonally averaged values of SUHI and SUHS intensity and the differences between the urban LCZs in Dubai.

4.1.1. Daytime Surface Urban Heat Sink

The daytime LST variations detected at 11 a.m. and 2 p.m. (GST) are shown in Fig. 6 for the urban LCZs and desert sand zone in Dubai. The LST variations for both times of day were consistent, with peaks of temperature observed especially during summer months (June, July and August). However, the afternoon LST measurements are higher than mornings by 3-5°C for all urban LCZs. The highest monthly average LST for urban LCZs was observed in August at 11 a.m. (approx. 44°C) and in July at 2 p.m. (approx. 49°C). The lowest LSTs were observed during

winter months (January, February and December) with afternoon temperature values higher than morning temperature values by 1-3°C. The desert sand LCZ shows the highest LST values during most of the year at both times of day with the highest values in the afternoon.

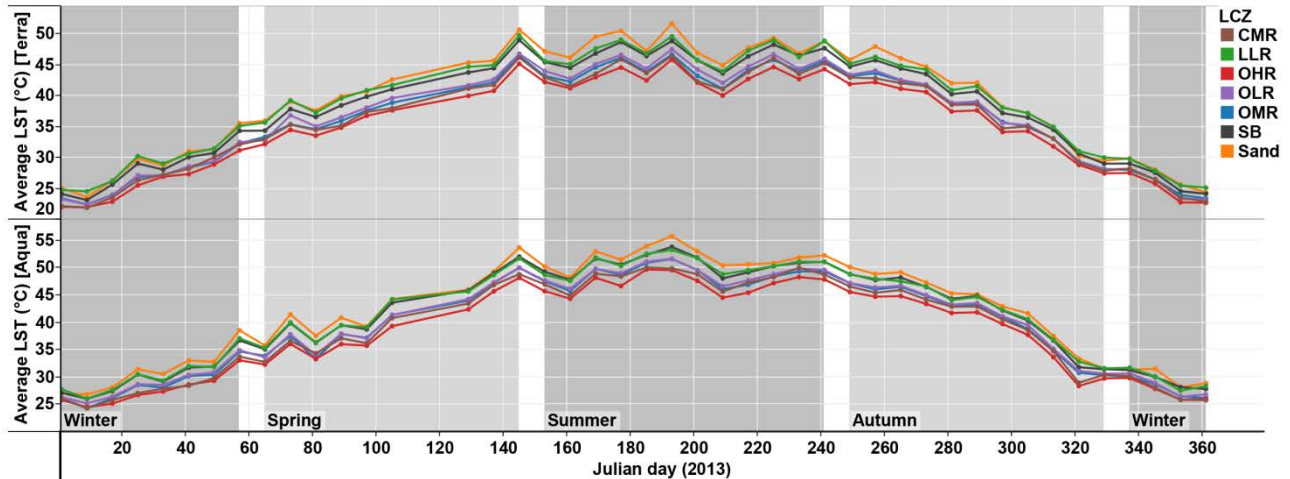


Figure 6. Daytime 8-day LST variations amongst LCZs at 11 a.m. (above) and 2 p.m. (below) GST, 2013.

Analysis of ΔLST at 11 a.m. and 2 p.m. revealed negative values which represent a SUHS during the daytime for the urban LCZs (Fig. 7), with the exception of some time periods in both the SB and LLR zones. Furthermore, the monthly averaged data (Fig. 8) clearly indicates that there are substantial differences between the LCZ classes in the magnitude of the SUHS at both times of day, though there is less contrast between SB and LLR zones at 2 p.m. Figure 8 also shows that the most intense SUHS occurred in June at 11 a.m. and in July at 2 p.m., while the weakest SUHS intensities occurred mainly during winter months.

The average seasonal and annual magnitude of the SUHS effect for urban LCZs is shown in Fig. 9. Annually, the SUHS was greater in the morning than the afternoon by an average cooling difference of 0.5°C. With the exception of LLR zones, the seasonal average SUHS intensity at 11 a.m. was greater than the SUHS at 2 p.m. for all LCZs with the highest intensity in summer by -3°C and lowest in winter by -1.8°C. The results show that the OHR and CMR

zones generated the most intense SUHS while the weakest effects were seen in the SB and LLR zones. The variations in SUHS between seasons and LCZs derived from the Landsat data (10:40 a.m.) (Fig.10) were very similar to variations observed using the MODIS Terra (11 a.m.) data (Fig.9, left graph). This demonstrates that despite the lower spatial resolution of MODIS data, they are still capable of representing the spatial variations in the SUHS phenomena and its response to LCZ characteristics, reinforcing the applicability of this data source for the majority of the analysis in this study.

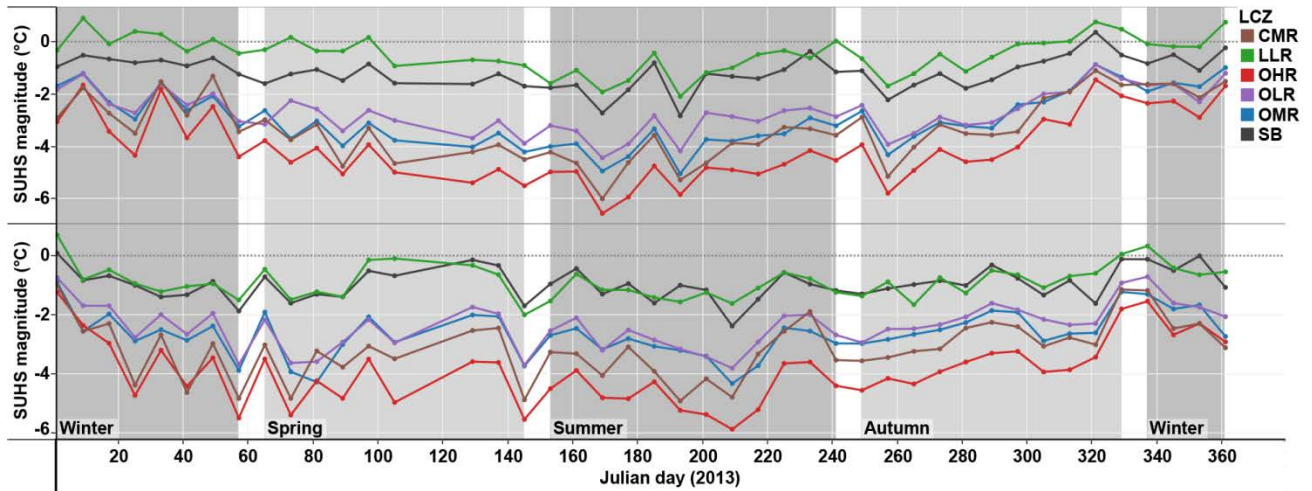


Figure 7. Daytime 8-day SUHS magnitude based on the relative difference between urban LCZs and desert sand at 11 a.m. (above) and 2 p.m. (below) GST, 2013.

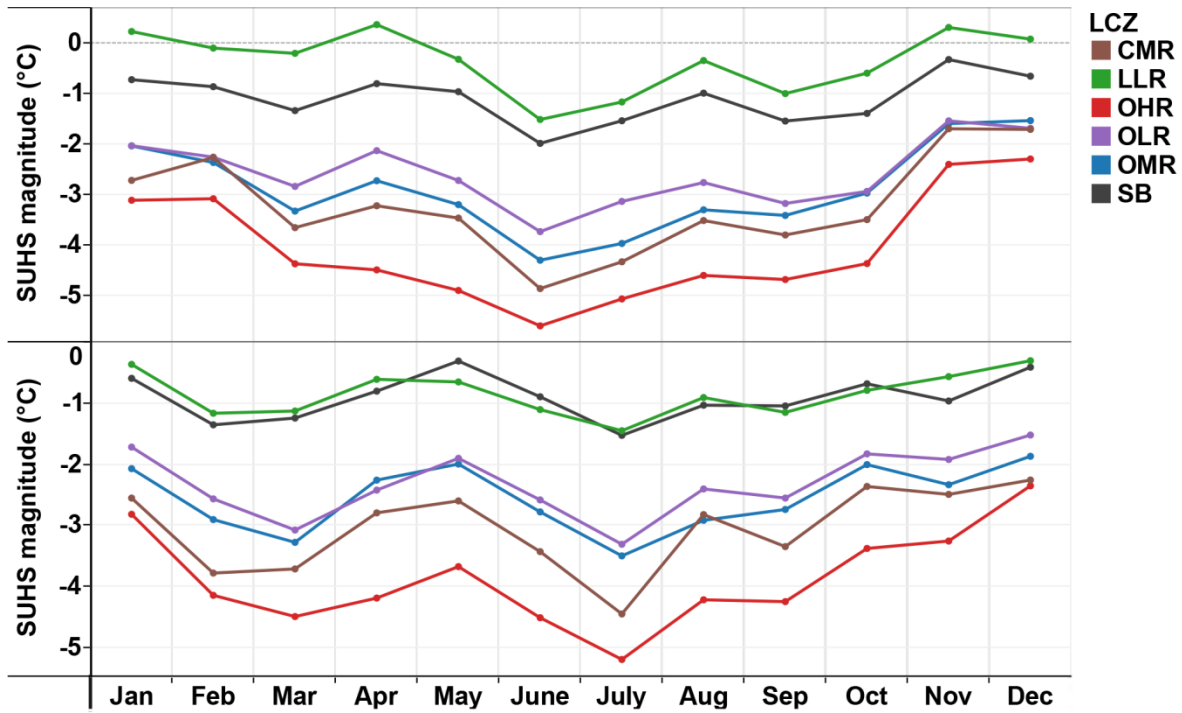


Figure 8. Daytime monthly average SUHS based on the relative difference between urban LCZs and desert sand at 11 a.m. (above) and 2 p.m. (below) GST, 2013.

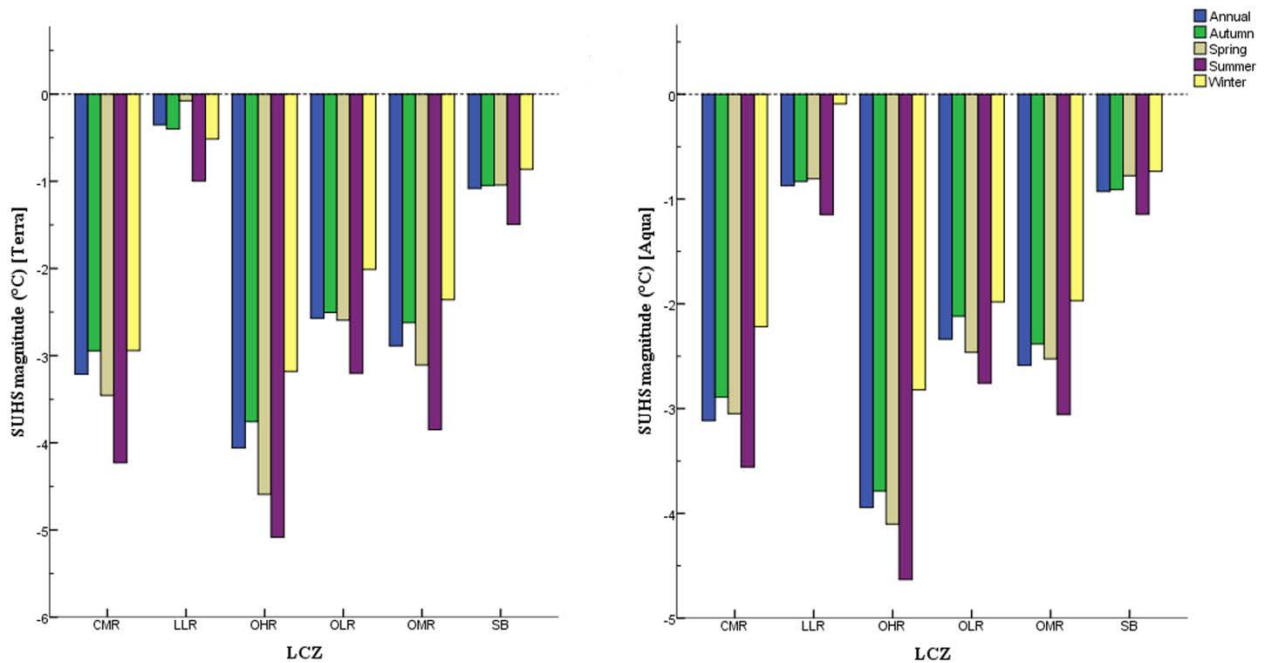


Figure 9. Daytime seasonal and annual average SUHS based on the relative difference between urban LCZs and desert sand at 11 a.m. (left) and 2 p.m. (right) GST, 2013.

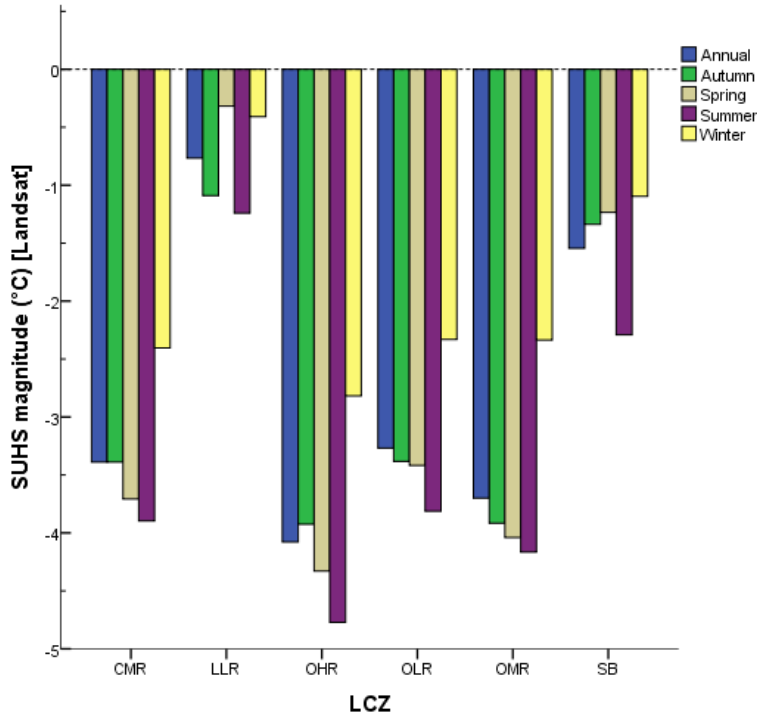


Figure 10. Daytime seasonal and annual average SUHS based on the relative difference between urban LCZs and desert sand at 10:40 a.m. GST as derived from Landsat 8 TIRS data, based on nine scenes from 2013.

4.1.2. Night-time Surface Heat Island

The night-time LST variations detected at 11 p.m. and at 2 a.m. GST are shown in Fig. 11 for the urban LCZs and desert sand zone in Dubai. Similar to the daytime observations, the highest LST values occurred during summer months (June, July and August) while the lowest values occurred during winter months (January, February and December). In contrast to daytime LST values, the desert sand zone exhibited lower LST than the urban LCZs at night while the CMR zone experienced the highest LST values throughout the year. The LLR zone experienced the lowest LST values amongst the urban LCZs. The LST values at 11 p.m. were higher than at 2 a.m. by 1-2.5°C during the summer months and 2-4°C during the winter months. The highest LST for urban LCZs at both times of night were observed in August and the lowest LST values for urban LCZs were found in January.

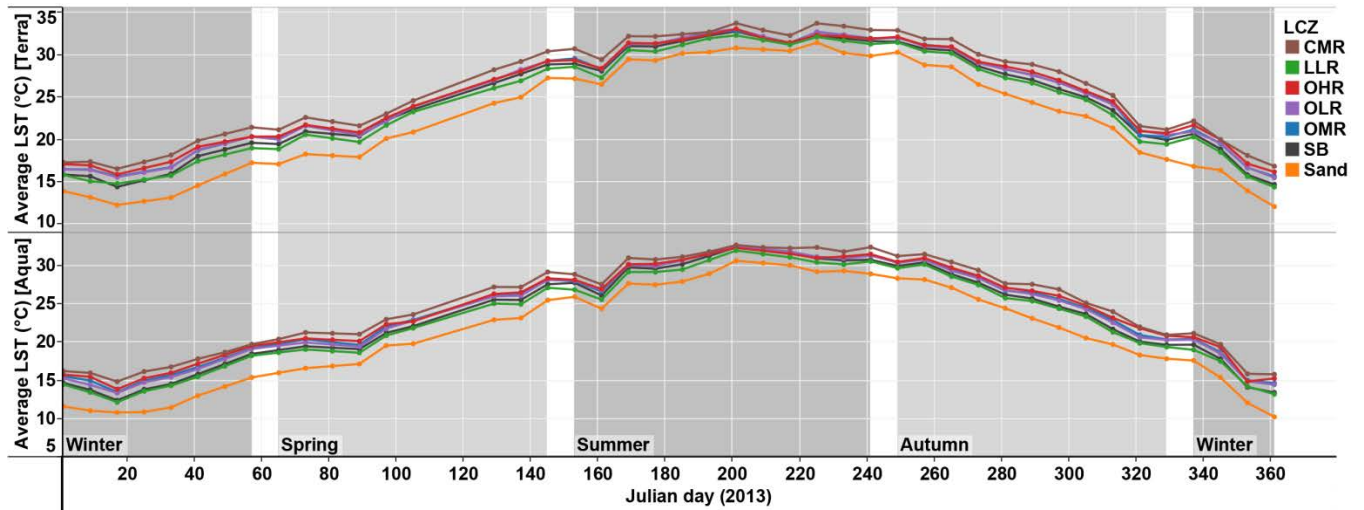


Figure 11. Night-time 8-day LST variations amongst LCZs at 11 p.m. (above) and 2 a.m. (below) GST, 2013.

A night-time SUHI was found for all of the urban LCZs, where all LST values were higher than that of the desert sand zone (Figure 12). The CMR zone shows the highest SUHI intensity throughout the year while the LLR zone consistently experienced the lowest SUHI intensity. Contrary to the SUHS, the weakest SUHI effect was observed in the summer while the strongest effect was found during the winter. Furthermore, the monthly SUHI intensities for the OHR, OMR and OLR zones show greater similarity during the summer months than winter months while other LCZs show clear contrasts throughout the year (Fig. 13).

The average seasonal and annual magnitude of the SUHI effect for urban LCZs is shown in Fig. 14. Annually, the SUHI was higher at midnight than the evening by an average difference of 0.2°C. The seasonal and annual averages of SUHI intensity were higher at 11 p.m. than 2 a.m. for all LCZs with the highest intensities in winter by 3.5°C and lowest in summer by 2°C. The major contributors to the SUHI effect were the CMR, OHR, OMR and OLR zones while the lowest contributions were by the LLR and SB zones.

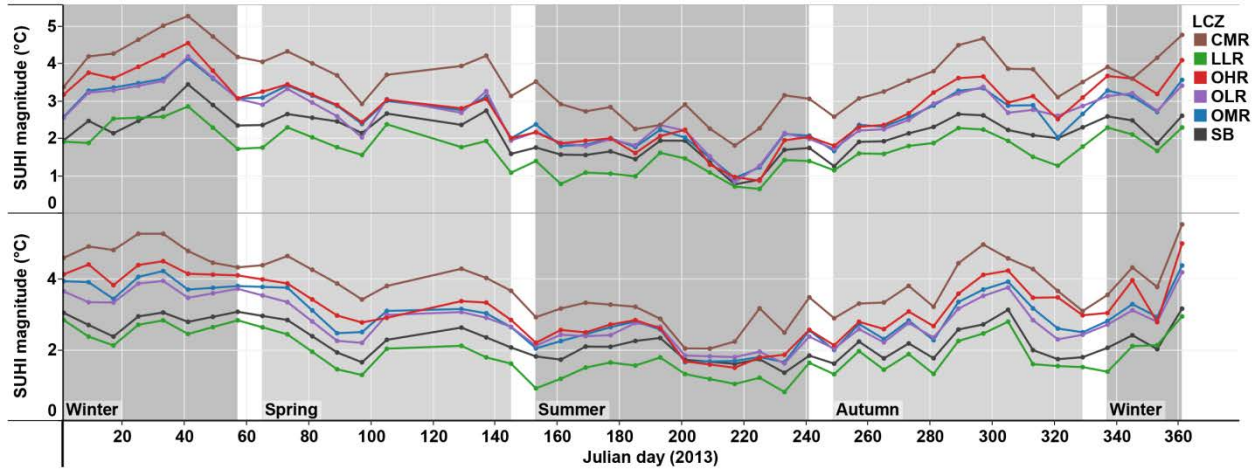


Figure 12. Night-time 8-day SUHI magnitude based on the relative difference between urban LCZs and desert sand at 11 p.m. (above) and 2 a.m. (below) GST, 2013.

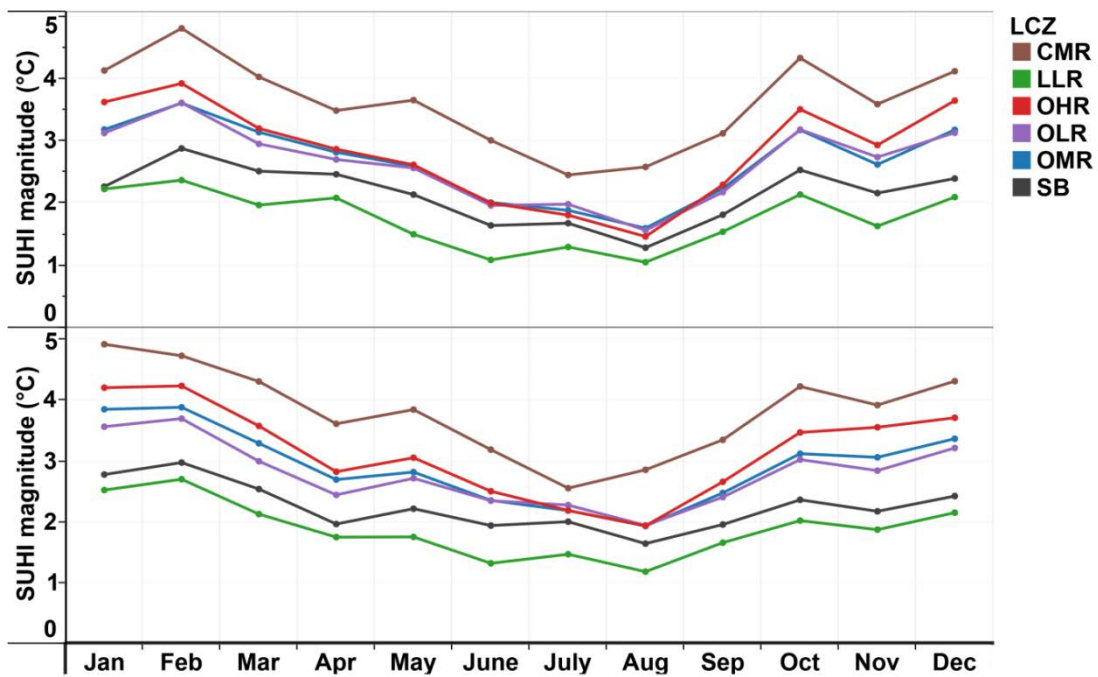


Figure 13. Night-time monthly average SUHI based on the relative difference between urban LCZs and desert sand at 11 p.m. (above) and 2 a.m. (below) GST, 2013.

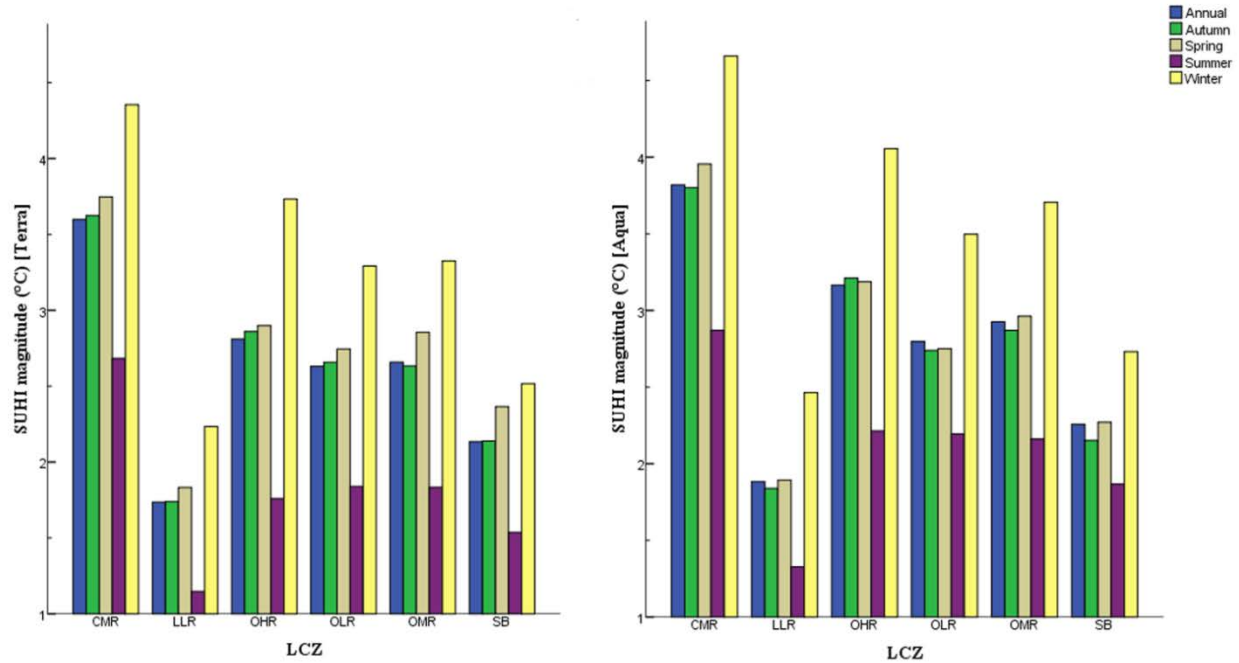


Figure 14. Night-time seasonal and annual average SUHI based on the relative difference between urban LCZs and desert sand at 11 p.m. (left) and 2 a.m. (right) GST, 2013.

4.2. Factors Influencing SUHS and SUHI Variations in Dubai

Our next objective was to investigate the correlation between a set of predictor physical variables and a set of criterion variables describing the SUHS and SUHI effects. Summer and winter seasons were selected for the analysis because, as demonstrated above, these seasons experienced either the highest or the lowest SUHS and SUHI effects, respectively.

The number of canonical correlations produced will be equal to the number of variables in the smaller data set of the predictor or criterion variables. Consequently, not all of the canonical correlations produced from a particular data are likely to be statistically significant. Furthermore, in order to interpret the meaning of the correlations between the two sets, the loading of each variable is used, which is similar to that for factor analysis loadings. Although there are no specific rules for selecting which loading values are important, in our interpretation it

may be reasonable to consider loadings below .40 as insignificant to weak, .41 to .70 as moderate and above .70 as strong (Laessig and Duckett, 1979).

4.2.1. Factors Influencing Daytime SUHS Variations in Dubai

As shown in Table 4, only one significant canonical correlation was produced in relation to the SUHS intensity at 11 a.m. and one for 2 p.m., according to the Chi-square significance values (i.e. values for the 2nd canonical correlation are insignificant for both times of day). For the significant correlations there was an identical correlation coefficient but higher % variability at 2 p.m. than 11 a.m. For both times of day, the first linear combination of physical predictors loaded strongly negative on proximity to the ocean, but with a higher magnitude at 2 p.m.. All of the urban geometry variables (HRE, SVF and BHV) were more highly loaded than land cover variables for both times of day. At both times of day the HRE and BHV variables loaded moderately positive, while SVF loaded moderately negative. The influence of the land cover variables varied with time of day, as VF loaded moderately positive at 11 a.m. but was weaker at 2pm while ISF loaded moderately negative at 2 p.m. but was very weak at 11 a.m. The remaining variables BSF and SandF had little or no contribution to SUHS intensity at either time of day. Finally, summer SUHS loaded higher than winter SUHS for both times of day, indicating that the combined physical variables are more predictive of SUHS variations during summer.

Table 4.

Canonical correlations between physical variables and daytime SUHS variations during summer and winter seasons at 11 a.m. and 2 p.m.

	Canonical solution for predicting daytime SUHS (11 a.m.)		Canonical solution for predicting daytime SUHS (2 p.m.)	
	1 st can. Corr.	2 nd Can. Corr.	1 st can. Corr.	2 nd Can. Corr.
Canonical correlation Coefficient	.88	.70	.88	.55
Chi-square significance	.0001	.165	.0001	.0832
Variability (%)	61.50	38.50	73.97	26.03
	Loadings			
<i>Predictor variables</i>				
HRE	.58	.29	.60	.43
BSF	.24	-.39	.25	.21
SVF	-.65	-.28	-.64	-.38
BHV	.61	.16	.56	.48
ISF	-.07	-.47	-.41	-.23
VF	.44	-.09	.37	.12
SandF	-.27	-.07	-.17	-.04
Proximity to the ocean	-.82	-.21	-.92	.14
<i>Criterion Variables</i>				
Summer SUHS	.95	.32	.99	.12
Winter SUHS	.83	.68	.64	.81

Note: n=39.

4.2.2. Factors Influencing Night-time SUHI Variations in Dubai

According to Table 5, only one significant canonical correlation was produced for Terra (11 p.m.) and Aqua (2 a.m.) data according to Chi-square significance values. The correlation coefficients for both night-time periods are lower than the correlations during both daytime periods which indicates that the correlation between the two set of predictor and criterion variables are weaker during night-time. Furthermore, the influence of urban geometry and proximity to the ocean on LST variations is inverted during night-time.

Similarly to daytime, proximity to the ocean and urban geometry variables had the highest loading. At 11 p.m., the first linear combination of physical predictors loaded strongly and negatively on proximity to the ocean and SVF while proximity to the ocean loaded strongly and SVF loaded moderately at 2 a.m. With the exception of ISF (which is already insignificant),

all loadings at 2 a.m. were lower in magnitude than 11 p.m. This indicates a weaker influence of these variables on the SUHI variations at 2 a.m. than 11 p.m. In contrast to the daytime, the loadings for winter LST were higher than summer SUHI for both time periods, indicating that the physical variables are more predictive of the SUHI variations during winter.

Table 5.
Canonical correlations between Physical variables and night-time SUHI variations during summer and winter at 11 p.m. and 2 a.m.

	Canonical solution for predicting night-time SUHI (11 p.m.)		Canonical solution for predicting night-time SUHI (2 a.m.)	
	1 st can. Corr.	2 nd Can. Corr.	1 st can. Corr.	2 nd Can. Corr.
Canonical correlation Coefficient	.74	.57	.71	.57
Chi-square significance	.0001	.082	.0001	.070
Variability (%)	63.02	36.98	60.43	39.57
	Loadings			
<i>Predictor variables</i>				
HRE	.60	-.10	.52	-.09
BSF	.33	.24	.31	.08
SVF	-.75	-.08	-.57	.29
BHV	.15	-.37	.11	.02
ISF	.12	.28	-.18	.45
VF	-.23	-.41	-.21	-.23
SandF	-.28	-.14	-.05	-.28
Proximity to the ocean	-.87	-.08	-.78	.51
<i>Criterion Variables</i>				
Summer SUHI	.40	.91	.75	.66
Winter SUHI	.87	.50	.91	.42

Note: n=39.

5. Discussion

The urban geometry and land cover properties that were utilized to classify Dubai's urban environment into LCZs have effectively characterized the landscape into units that have distinct thermal responses diurnally and seasonally. As expected, the SUHS phenomenon was observed during the daytime while the SUHI phenomenon was noted during the night for the majority of LCZs. One reason these phenomena exist might relate to differences in specific heat capacity

between the urban materials of the LCZs and the natural sands of the desert. Indeed, the specific heat capacity for typical urban surface materials such as asphalt, aluminum, concrete and bricks is higher than that of sand (Physics Hypertextbook, 2014). This means that sand shows a larger increase in LST than the urban surfaces during the daytime (Fig. 6) and a larger decrease in LST than the urban surfaces during the night (Fig. 11).

The differences in magnitudes of SUHS and SUHI depending on LCZ type, time of the day and season, suggest that the properties used to characterize the LCZs influence the LST variations differently. The SUHS was stronger for zones with medium to high-rise buildings, thus these zones are most advantageous for daytime cooling (Figs. 7-10). However, during the night the SUHI was higher in zones with medium to high-rise buildings, with the highest intensity in compact-midrise zones, and the least intense SUHI in the sparsely built and large low-rise zones (Figs. 12-14). This indicates that some or all of the LCZs' properties (Table 2) can result in the urban environment exhibiting quite different thermal behavior depending on the stage of the diurnal cycle.

The findings indicate that the SUHS effect is greater in summer than winter, while the SUHI is greater in winter than summer. The reasons for this are somewhat unclear, but as windspeed and humidity vary little with seasons in Dubai and air temperature varies considerably, radiation and thermal effects may be the key factors controlling the SUHS and SUHI seasonal dynamics. It may be that in summer during the period of maximum solar radiation the effects of surface shading by buildings generates a proportionally larger reduction in urban LST relative to surrounding desert (a higher SUHS) than in winter when radiation is less intense and the desert experiences less solar heating (see Littlefair et al., 2000). Likewise, with lower daytime heating of the desert in winter, night-time LST is lower in winter than summer and because of the

differences in specific heat capacity of sand and urban materials (mentioned above) and the continued contribution to urban heating from anthropogenic sources during winter, the SUHI may be greater in winter. However, while these are feasible mechanisms, the reasons for the seasonal dynamics of SUHS and SUHI do require further investigation.

The multivariate correlation analyses (Tables 4 and 5) revealed that proximity to the ocean and differences in urban geometry explain most of the variation in SUHI and SUHS intensity. This finding underscores the importance of integrating urban geometry into urban heat studies (Hwang et al., 2011; Voogt and Oke, 2003) and emphasizes the importance of including proximity to large water bodies as an essential factor in urban heat studies, being particularly relevant for coastal cities.

During daytime, proximity to the ocean contributed strongly and negatively to the SUHS which indicates that zones closer to the coast exhibit larger SUHS (cooling). This influence is due to the presence of sea-breeze which helps in cooling nearby urban surfaces, with a larger effect at 2 p.m. than 11 a.m. Indeed, at 2 p.m. and especially during the summer season, the solar radiation increases to its maximum thus the temperature contrast between the land and ocean is greatest which promotes a stronger sea-breeze (Dailey and Fovell, 1999). These findings also concur with Coseo and Larsen (2014) who reported that breezes from Lake Michigan cooled urban areas that were nearer to the shoreline. However, building heights (HRE) loaded positively with SUHS variations and this is likely to be a result of taller buildings producing greater shadows which reduce the amount of solar energy reaching the land surface thus increasing the cooling of urban areas (e.g. Kato et al., 2010). Similarly, building height variations (BHV) loaded positively with SUHS, this may be explained by buildings with larger height variations producing stronger surface wind circulation thus helping to cool urban surfaces (Johansson and

Emmanuel, 2006) and this could also be related to greater land surface shadowing in areas with larger BHV. On the other hand, SVF loaded negatively with SUHS variations, which indicates that a lower SVF leads to fewer urban surfaces that are exposed to incoming solar radiation thereby increasing the SUHS effect.

At 11 a.m. the magnitude of the SUHS was higher than at 2 p.m. and this finding was consistent across most urban LCZs and seasons (Fig. 9). This is likely due to the greater influence of impervious surface fraction (ISF), as a heat source, at 2 p.m. compared to 11 a.m., evidenced by the stronger loading. The greater influence of ISF at 2 p.m. is related to the fact that the impervious surfaces of roads, walkways and parking lots have higher LST than 11 a.m. due to longer period of exposure to solar radiation. In addition, the vegetation fraction (VF), as a cooling source, has a slightly more influence on SUHS at 11 a.m. than 2 p.m. with higher loading at 11 a.m. This might be related to the irrigation time of vegetated areas which usually occurs in the early mornings, therefore the quantity of water in vegetated areas can be lost to evaporation at 2 p.m. much larger than 11 a.m.

The variations between the characteristics of the different LCZs are illustrated in Figure 9 and Tables 2 & 3. Open high-rise zones (OHR) and compact mid-rise zones (CMR) showed higher SUHS than other zones due to the effects of their urban geometry (see Fig. 5), evidenced by the moderate loadings of three geometry properties in the canonical regression (Table 4). The tall buildings in OHR and narrow streets in CMR zones are likely to generate relatively greater shadow than other LCZs especially during the sun peak hours thus exhibiting more cooling (Littlefair et al., 2000). The effect of urban geometry on the SUHS is further demonstrated by the finding that open mid-rise (OMR) zones have a higher SUHS than open low-rise (OLR) zones. OLR zones are characterized by smaller values of HRE and BHV and larger SVF, therefore the

effect of shadow is minimized and the incoming solar radiation is larger compared to OMR zones. In addition to the urban geometry, other factors might have also contributed to the SUHS variations. For example, in the LLR zones the industrial activities and the metal construction materials with lower specific heat capacities than other urban materials may explain why this LCZ had the lowest SUHS effect.

Proximity to the ocean strongly and negatively influenced night-time SUHI variations (Table 5). This may be explained by areas close to the ocean experiencing a more intense land-breeze cooling during the night than areas further inland (Freitas et al., 2007). Similarly, SVF had a strong negative influence on SUHI indicating that the zones with lower SVF exhibit a higher SUHI effect. During the night-time, a low SVF increases radiative heat trapping within urban areas thus increasing the SUHI intensity (Wong et al., 2011). HRE had a moderate positive influence on SUHI variations again suggesting that the presence of taller buildings increases the radiative heat trapping effect at night.

These findings are supported when we look at the variations between LCZs in SUHI dynamics (Figure 14 and Tables 2&3). The CMR and OHR zones exhibited the highest SUHI intensities and are characterized by their tall buildings and lower SVFs compared to other zones. As indicated above taller buildings with low SVF trap radiative heat near the surface at night thereby enhancing SUHI intensity. Furthermore, the LLR zones exhibited the lowest night-time SUHI which may be attributed to the metal construction materials that dominate this zone, which have a low specific heat capacity and lose heat at a higher rate at night than the construction materials in other SB zones.

In Dubai, the unbuilt surfaces of LCZs are still covered mainly by sand while vegetation and inland water cover less than 5% of the studied LCZs. It is important to mention that the vast

majority of vegetation cover is found in parks, farms and golf courses which contain a very limited amount of impervious surfaces and buildings (Nassar et al., 2014), thus these areas were not selected in the LCZ classification process, as per the classification system of Stewart and Oke (2012). This might explain the low contribution VF of as a predictor of SUHS and SUHI variability found in the statistical analysis (Tables 4 & 5).

Finally, in considering the findings for both SUHS and SUHI dynamics together, it can be seen that urban geometry can have both beneficial and negative impacts on the thermal characteristics of LCZs in Dubai, from the perspective of human habitation of these environments. For example, geometries that generate shadow effects which decrease the absorption of solar energy and increase wind speeds and natural ventilation at street level lead to beneficial cooling of urban surfaces during daytime. However, during the night, the same urban geometries can trap heat near to the surface resulting in a detrimental heating effect. Identifying urban geometries which balance appropriately these beneficial and negative impacts in the prevailing climatic conditions of desert environments should be a key focus for future research.

6. Conclusions

The main aim of this study was to elucidate the dynamics and controls of SUHS and SUHI phenomena in Dubai using MODIS thermal imagery and an LCZ-based sampling strategy. We have systematically analyzed how various urban zones with varying structures, cover types and proximity to the ocean influence urban cooling and heating in the desert city of Dubai. This provides a valuable extension to previous studies in coastal desert cities which have considered only land cover factors (Frey et al., 2007; Lazzarini et al., 2013).

In terms of the SUHS and SUHI intensities, we have found that different LCZs exhibited different responses in intensity, both diurnally and seasonally, which clearly indicates that the predictor variables affecting those intensities behave differently. On average, we found that the summer daytime SUHS magnitude was significantly higher than other seasons and that the winter daytime SUHS was the lowest. Conversely, during the night-time, winter SUHI magnitude was significantly higher than other seasons while summer night-time SUHI was the lowest. We have demonstrated that proximity to the ocean, sky view factor, height of roughness elements and building height variations are the major factors governing the zonal SUHS and SUHI variations in Dubai.

To further investigate the factors influencing the surface thermal variation of LCZs, we encourage other researchers to use other LCZ characteristics such as traffic loads, anthropogenic activities, wind speed and albedo.

Acknowledgements

The authors would like to thank U.S. Geological Survey for providing the free MODIS and Landsat data and Dubai governmental departments for providing the other spatial datasets. We also thank the editor and the two anonymous reviewers for their constructive comments.

References

- Alexander, P.J., & Mills, G., 2014. Local Climate Classification and Dublin's Urban Heat Island. *Atmosphere*, 5 (4), 755-774. doi: 10.3390/atmos5040755
- Bechtel, B., & Daneke, C., 2012. Classification of local climate zones based on multiple earth observation data. *Selected Topics in Applied Earth Observations and Remote Sensing*, IEEE Journal 5(4), 1191-1202. doi: 10.1109/JSTARS.2012.2189873
- Coseo, P., & Larsen, L., 2014. How factors of land use/land cover, building configuration, and adjacent heat sources and sinks explain Urban Heat Islands in Chicago. *Landscape and Urban Planning*, 125, 117–129. doi: 10.1016/j.landurbplan.2014.02.019
- Coutts, A., & Harris, R., 2012. *Urban Heat Island Report: A multi-scale assessment of urban heating in Melbourne during an extreme heat event: policy approaches for adaptation*. Victorian Centre for Climate Change Adaptation Research.
- Cui, Y.Y., & Foy, D.E., 2012. Seasonal variations of the urban heat island at the surface and the near-surface and reductions due to urban vegetation in Mexico City. *Journal of Applied Meteorology and Climatology*, 51(5), 855-868. doi: 10.1175/JAMC-D-11-0104.1
- Dailey, P.S., & Fovell, R.G., 1999. Numerical simulation of the interaction between the sea-breeze front and horizontal convective rolls. part 1: offshore ambient flow. *American Meteorological Society*, 127, 858-878. doi: [http://dx.doi.org/10.1175/1520-0493\(1999\)127<0858:NSOTIB>2.0.CO;2](http://dx.doi.org/10.1175/1520-0493(1999)127<0858:NSOTIB>2.0.CO;2)
- Dubai Statistical Centre, 2014. Population Bulletin: Emirates of Dubai. <https://www.dsc.gov.ae/en-us/Themes/Pages/Climate-and-Environment.aspx?Theme=35> (accessed 9th May, 2015).
- Dubai Statistical Centre, 2013. Population Bulletin: Emirates of Dubai. <https://www.dsc.gov.ae/en-us/Themes/Pages/Population-and-Vital-Statistics.aspx?Theme=42> (accessed 23rd June, 2015).
- Elsheshtawy, Y., 2010. *Dubai: Behind an Urban Spectacle*. Routledge; 1 ed. Oxfordshire.
- Emmanuel, R., & Kruger, E., 2012. Urban heat island and its impact on climate change resilience in a shrinking city: The case of Glasgow, UK. *Building and Environment*, 53, 137-149. doi:10.1016/j.buildenv.2012.01.020
- Freitas, E., Rozoff, C., Cotton, W., & Dias, P., 2007. Interactions of an urban heat island and sea-breeze circulations during winter over the metropolitan area of São Paulo, Brazil. *Boundary-Layer Meteorology*, 122(1), 43-65. doi: 10.1007/s10546-006-9091-3
- Frey, C. M., Rigo, G., & Parlow, E., 2007. Urban radiation balance of two coastal cities in a hot and dry environment, *International Journal of Remote Sensing*, 28(12), 2695-2712. <http://dx.doi.org/10.1080/01431160600993389>
- Gartland, L., 2008. *Heat Islands: Understanding and mitigating heat in urban areas*. Washington, DC: Earthscan.
- Guarino, J., 2004. A comparison of first and second generation multivariate analyses: canonical correlation analysis and structural equation modeling. *Florida Journal of Educational Research*, 42, 22 – 40.
- Heldens, W., Taubenböck H., Esch T., Heiden U., & Wurm M., 2013. Analysis of surface thermal patterns in relation to urban structure types: a case study for the city of Munich. In: Kuenzer C., &

- Dech S. (eds). *Thermal infrared remote sensing – sensors, methods, applications. Remote sensing and digital image processing series 17*. Springer, Netherlands, p. 475–495.
- Hwang, R-L., Lin, T-P., Lin, T-P., & Matzarakis, A., 2011. Seasonal effects of urban street shading on long-term outdoor thermal comfort. *Building and Environment*, 46, 863-870. doi: 10.1016/j.buildenv.2010.10.017
- Imhoff, M.L., Zhang, P., Wolfe, R.E., & Bounoua, L., 2010. Remote sensing of the urban heat island effect across biomes in the continental USA. *Remote Sensing of Environment*, 114, 504–513. doi: 10.1016/j.rse.2009.10.008
- Johansson, E., & Emmanuel, R., 2006. The influence of urban design on outdoor thermal comfort in the Hot Humid City of Colombo, Sri Lanka. *International Journal of Biometeorology*, 51, 119-133. doi: 10.1007/s00484-006-0047-6
- Johnson, G.T., & Watson, I.D., 1984. The determination of view-factors in urban canyons. *Journal of Climate and Applied Meteorology*, 23, 329–335. doi: [http://dx.doi.org/10.1175/1520-0450\(1984\)023<0329:TDOVFI>2.0.CO;2](http://dx.doi.org/10.1175/1520-0450(1984)023<0329:TDOVFI>2.0.CO;2)
- Kato, S., & Yamaguchi, Y., 2005. Analysis of urban heat-island effect using ASTER and ETM+ data: Separation of anthropogenic heat discharge and natural heat radiation from sensible heat flux. *Remote Sensing of Environment*, 99, 44–54. doi: 10.1016/j.rse.2005.04.026
- Kato, S., Matsunaga, T., & Yamaguchi, Y., 2010. Influence of shade on surface temperature in an urban estimated by ASTER data. *International Archives of the Photogrammetry, Remote Sensing and Spatial Information Science*, 38, 925–929.
- Knight, S., Claire, S., & Michael, R., 2010. Mapping Manchester's urban heat island. *Weather*, 65(7), 188-193. doi: 10.1002/wea.542
- Laessig, R. E., & Duckett, E. J. 1979. Canonical correlation analysis: potential for environmental health planning. *American journal of public health*, 69(4), 353-359.
- Lazzarini, M., Marpu, P.R., & Ghedira, H., 2013. Temperature-land cover interactions: The inversion of urban heat island phenomenon in desert city areas. *Remote Sensing of Environment*, 130, 136–152. doi: 10.1016/j.rse.2012.11.007
- Leconte, F., Bouyer, J., Claverie, R., & Pétrissans, M., 2015. Using Local Climate Zone scheme for UHI assessment: Evaluation of the method using mobile measurements. *Building and Environment*, 83, 39-49. doi: 10.1016/j.buildenv.2014.05.005
- Lelovics, E., Unger, J., Gál, T., Gál, & C.V., 2014. Design of an urban monitoring network based on Local Climate Zone mapping and temperature pattern modelling. *Climate Research*, 61(1), 51-62. doi:10.3354/cr0122
- Littlefair, P.J., Santamouris, M., Alvarez, S., Dupagne, A., Hall, D., Teller, J., et al., 2000. *Environmental site layout planning: solar access, microclimate and passive cooling in urban areas* (1st ed.). Watford: CRC.
- Nassar, A.K., Blackburn, G.A., & Whyatt, J.D., 2014. Developing the desert: The pace and process of urban growth in Dubai. *Computers, Environment and Urban Systems*, 45, 50–62. doi: 10.1016/j.compenvurbsys.2014.02.005
- Obiakor, M.O.; Ezeonyejiaku, C.D. & Mogbo, T.C., 2012. Effects of Vegetated and Synthetic (Impervious) Surfaces on the Microclimate of Urban Area. *Journal of Applied Sciences and*

- Environmental Management*, 16(1), 85-94.
- Oda, R., & Kanda, M., 2009. Cooling effect of sea surface temperature of Tokyo bay on urban air temperature. *The seventh International Conference on Urban Climate*, 1-4, 29 June - 3 July 2009, Yokohama, Japan.
- Physics Hypertextbook, 2014. <http://physics.info/heat-sensible/> (accessed 1st February, 2014).
- Pichierri, P., Bonafoni, S., & Biondi, B., 2012. Satellite air temperature estimation for monitoring the canopy layer heat island of Milan. *Remote Sensing of Environment*, 127, 130–138. doi: 10.1016/j.rse.2012.08.025
- Skyscraper Center, 2016. <http://skyscrapercenter.com/city/dubai> (accessed 1st March, 2016).
- Unger, J., 2009. Connection between urban heat island and sky view factor approximated by a software tool on a 3D urban database. *Int. J. Environment and Pollution*. 36, 59-80. doi: 10.1504/IJEP.2009.021817
- US EPA., 2008. Urban Heat Island basics. In *Reducing Urban Heat Islands: Compendium of Strategies*. Washington. <http://www.epa.gov/heatisland/resources/pdf/BasicCompendium.pdf> (accessed 8th June, 2013).
- USGS (U.S. Geological Survey), 2014. http://landsat.usgs.gov/calibration_notices.php. http://landsat.usgs.gov/calibration_notices.php (accessed 9th September, 2014).
- Rhee, J., Seonyoung, P., & Zhenyu, Lu., 2014. Relationship between land cover patterns and surface temperature in urban areas. *GIScience & Remote Sensing*, 51(5), 521-536. doi:10.1080/15481603.2014.964455
- Sattari, F., & Hashim, M., 2014. A brief review of land surface temperature retrieval methods from thermal satellite sensors. *Middle-East Journal of Scientific Research*, 22 (5), 757-768. doi: 10.5829/idosi.mejsr.2014.22.05.21934
- Siu, L.W., & Hart, M.A., 2013. Quantifying urban heat island intensity in Hong Kong SAR, China. *Environmental Monitoring and Assessment* 185, 4383–4398. doi: 10.1007/s10661-012-2876-6
- Stewart, I. D., & Oke, T. R., 2012. Local climate zones for urban temperature studies. *Bulletin of the American Meteorological Society*, 93(12), 1879-1900. doi: <http://dx.doi.org/10.1175/BAMS-D-11-00019.1>
- Stewart, I.D., Oke, T. R., & Krayenhoff, E. S., 2014. Evaluation of the ‘local climate zone’ scheme using temperature observations and model simulations. *International Journal of Climatology*, 34(4), 1062-1080. doi: 10.1002/joc.3746
- Tabachnick, B.G., & Fidell L.S., 2012. *Using Multivariate Statistics* (6 ed.). Boston: Pearson Education Inc.
- Voogt, J.A., & Oke, T.R. 2003. Thermal remote sensing of urban climates. *Remote Sensing of Environment*, 86, 370–384. doi: 10.1016/S0034-4257(03)00079-8
- Wan, Z., & Dozier, J., 1996. A generalized split-window algorithm for retrieving land-surface temperature from space. *IEEE Transactions on Geoscience and Remote Sensing*, 34(4), 892–905. doi: 10.1109/36.508406
- Weng, Q., 2001. A remote sensing-GIS evaluation of urban expansion and its impact on surface temperature in the Zhujiang Delta, China. *International Journal of Remote Sensing*, 22, 1999–2014.

doi: 10.1080/713860788

Wong, N.Y., Jusuf, S.K., Samsudin, R., & Ignatius, M., 2011. Urban morphology and temperature mapping comparative study Case study: Singapore's commercial area. *7th International conference on Passive and Low Energy Architecture*, 13-15 July, Louvaine La Nouve, Belgium.

Yuan, F., & Bauer, M.E., 2007. Comparison of impervious surface area and normalized difference vegetation index as indicators of surface urban heat island effects in Landsat imagery. *Remote Sensing of Environment*, 106, 375–386. doi: 10.1016/j.rse.2006.09.003.

Zakšek, K., Oštir, K., & Kokalj, Ž., 2011. Sky-View Factor as a Relief Visualization Technique. *Remote Sensing*, 12, 398-415. doi: <http://dx.doi.org/10.3390/rs3020398>